4 Experimental Tools in Nanophotonics II: Near-field Techniques

Highlights of this chapter: This chapter introduces scanning near-field optical microscopy, SNOM. Basics, trands, and applications are discussed.

4.1 Fundamentals of SNOM

In the theory chapter we found that spatial frequencies above a certain cut-off frequency, i.e., spatial information below a certain characteristic length are not transferred via the far-field of an electromagnetic wave. Instead, this information is contained in the near-field and "transported" via exponentially decaying evanescent fields.

There is an interesting analogy to *Heisenberg's uncertainty relation:*

- Let the image of an object be described via an intensity distribution of an electromagnetic field $I(x, y, z)$.

- A point $P = (x, y, z)$ (where the k-vector of the e.m.-field is $k = (k_x, k_y, k_z)$) can not be determined with arbitrary position, but only within the Heisenberg uncertainty:
$$\Delta x > 1/\Delta k_x = 1/2k_{x,\max} \qquad (239)$$

- If all components of k are real, then k_x is defined by the projection of k on the x-axis and it is:
$$k_x = |k| \sin \vartheta < k_{x,\max} = |k| \qquad (240)$$

- Therefore:
$$\Delta x > \lambda/(2n \sin \vartheta) \geq \lambda/2n \qquad (241)$$

The Abbe-Limit is a classical analogy to Heisenberg's uncertainty relation.

- In the general case k_x has to fulfill only
$$k_x = \sqrt{|k|^2 - k_y^2 - k_z^2} \qquad (242)$$

It can be arbitrarily large if k_y or k_z are complex, i.e., then also Δx can be arbitrarily small.

1928 E. H. Synge suggested a higher optical resolution by scanning across the *near-field* (E. H. Synge, Phil. Mag. 6, 356, (1928)). The following figure 72 illustrates his idea.
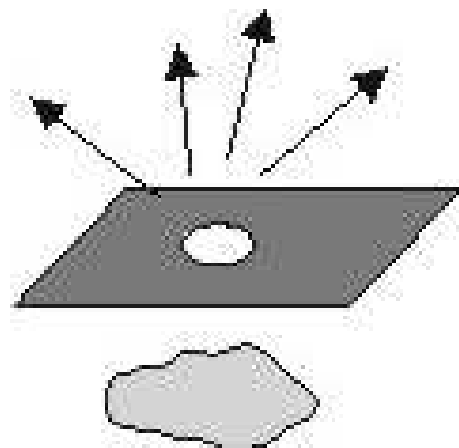
Figure 72: Cartoon picture of Synge's idea: A tiny aperture is scanned across an object and detects the optical near-field. A resolution below the Rayleigh limit is obtained in this way.
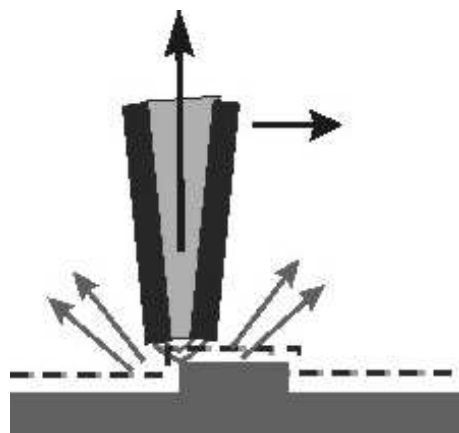
Figure 73: Principle of a modern realization of a SNOM aperture with the help of a metal coated optical fiber.

Similar as in confocal optical microscopy, the imaging via near-field detection is point-by-point. In order to obtain a complete image the object has to be scanned. Therfore: **Scanning Near-field Optical Microscopy, SNOM**.

Because of the experimental difficulties Synge's idea could not be realized and was somewhat forgotten. Only in the 70ies first near-field measurements were performed in the microwave domain.

In 1982 the group of Pohl at IBM Zürich was the first to perform experiments with visible light. This was the birth of *near-field optical microscopy*. The following figures 74 and 75 show a page from Pohl's lab book and the near-field image of a line grating (obtained resolution: $150\,nm$).
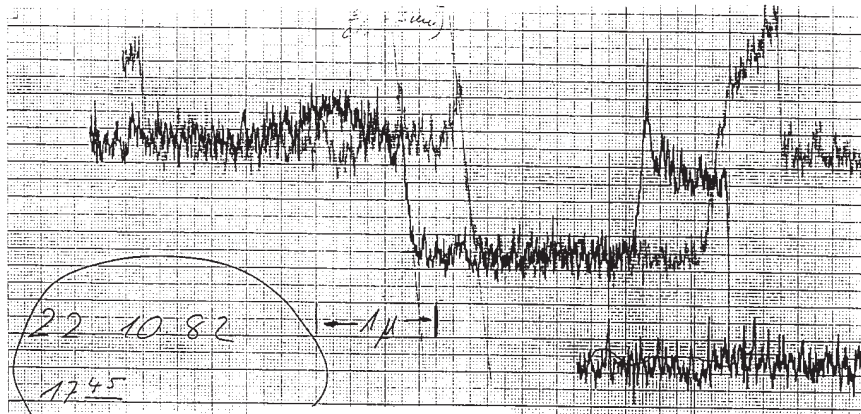
Figure 74: From Pohl's lab book in the year 1982. [from Paesler/Moyer "Near-Field Optics"]

Different realizations of near-field microscopy have one thing in common: There has to be scattering process which transfers non-propagating near-fields into propagating far-fields.
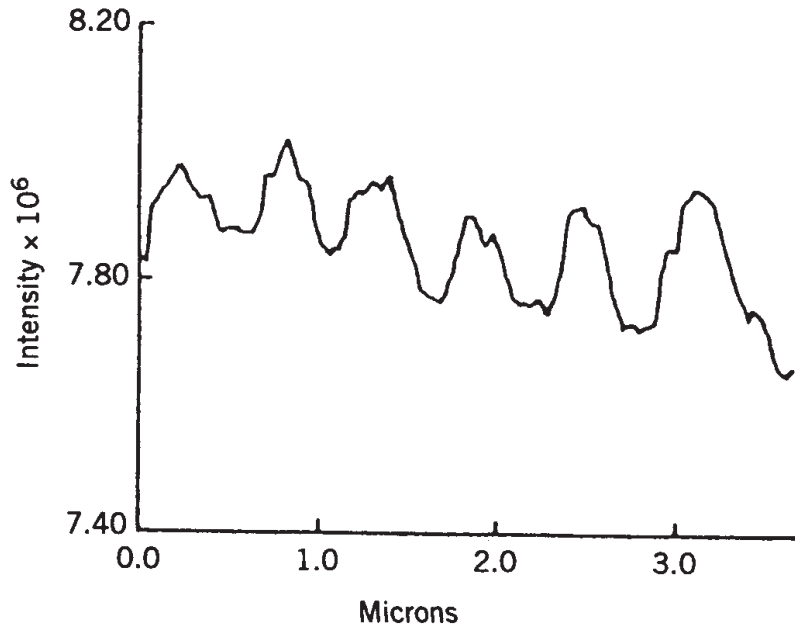
Figure 75: Intensity cross section of a line grating. [from Paesler/Moyer "Near-Field Optics"]

The following following figure 76 introduces three configurations of SNOM:
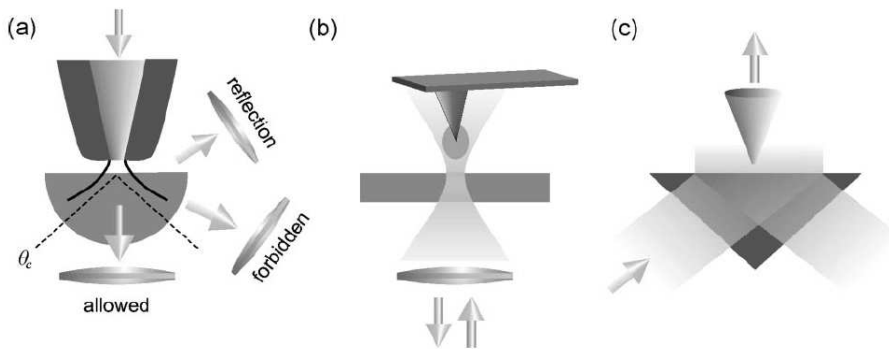
Figure 76: (a) aperture SNOM, (b) aperture-less SNOM, and (c) scanning tunneling microscopy. [from Hecht et al., J. Chem. Phys., 112, pp. 7761-7774 (2000)]

1. Aperture SNOM:
   The evanescent field at the end of a small aperature is locally scattered by an object. Detection of the scattered light is possible in the far-field.

2. Aperture-less SNOM:
   A tiny probe of sub-wavelength dimension locally scatters the near-fields of an illuminated object. The scattered light is detected by a far-field detector.

3. Scanning tunneling microscopy:
   An evanescent field is created on the surface of, e.g., a prism. This is scattered and detected by a probe.

Here we deal at first with **Aperture SNOM**. Aperture-less SNOM will be discussed further below in the subchapter "SNOM Trends".

The interpretation of SNOM images is complicated. Many approximations used in macroscopic optics are not valid as length changes on the order of the optical wavelength play an important role for image formation in SNOM. Simplified concepts based merely on reflection and transmission coefficients loose their meaning. The fundamental concept to treat the interaction between light and object is scattering.

An example for the peculiar interaction in the near-field is provided in the following figure 77 which shows the calculated intensity 4 nm above a sliver (dashed) and a glass wire of dimension 2 nm x 6 nm when illuminated by s-polarized light. Although silver has a much higher reflectivity than glass, there is a much smaller field right above the wire.
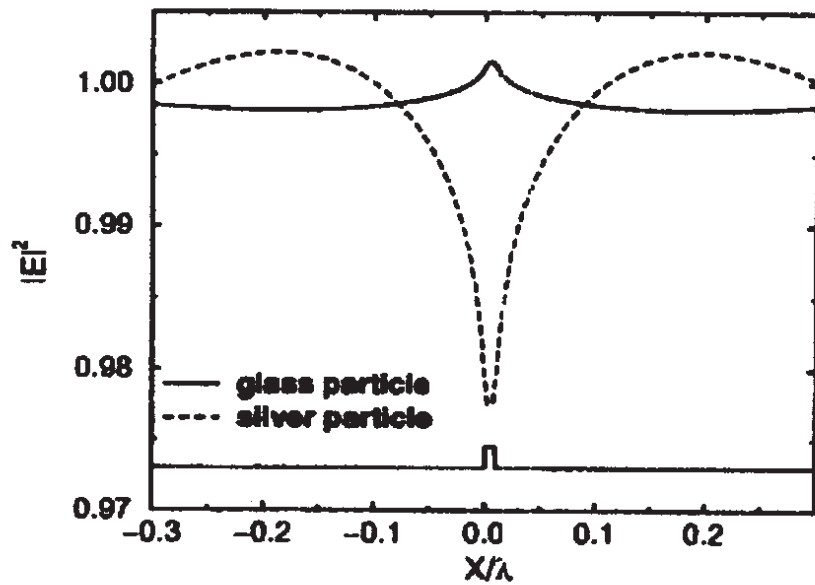
Figure 77: Calculated intensity $4\,nm$ above a $2 \times 6\,nm$ silver wire (dashed) and a glass wire (solid) [from Greffet, Carminati, Progr. Surf. Sci., 56, 133 (1997)]

The calculation of the expected image (e.g., in the example above) can be done in three steps:

1. Calculation of the intensity distribution at the SNOM aperture

2. Interaction (scattering) at the object

3. Integration and detection of the signal as a function of x, y, z

Already step 1 is non-trivial. Fresnel diffraction is not sufficient to treat diffraction at a sub-wavelength aperture. A treatment was derived in 1950 by Bouwkamp based on first results from Bethe. Bethe showed that the far-field emission of a small aperture is equivalent to the emission of an electric and magnetic dipole located at the position of the aperture. Bouwkamp solved the problem at first for a small disk and then applied the principle of Babinet to derive the fields for a small aperture. This approach is denoted as **Bethe-Bouwkamp-Theorie.**

The following figure 78 shows the intensity distribution of a aperture for linearly polarized (x-direction) light according to the Bethe-Bouwkamp-Theory. It is striking that also y -and z-components of the field appear.
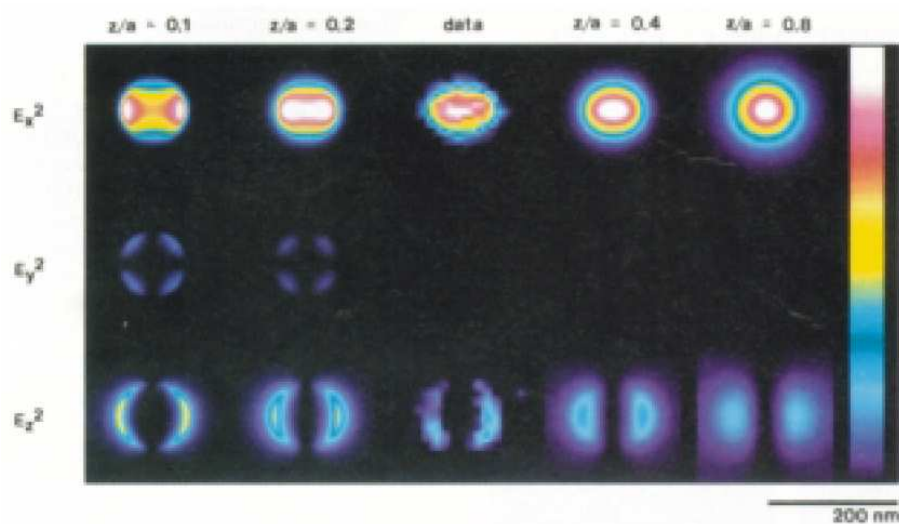
Figure 78: Calculated intensity of x-polarized light at a small aperture according to the Bethe-Bouwkamp-Theory (a=diameter of aperture, z=distance from aperture) [from Betzig, Chichester, Science 262, 1422 (1993)]]

For complex configurations numerical solutions are required. The following figure 79 shows the intensity in the near-field of an aperture above a perfectly conducting cylinder. The results were obtained by the multiple-multipole method in a 2D calculation.
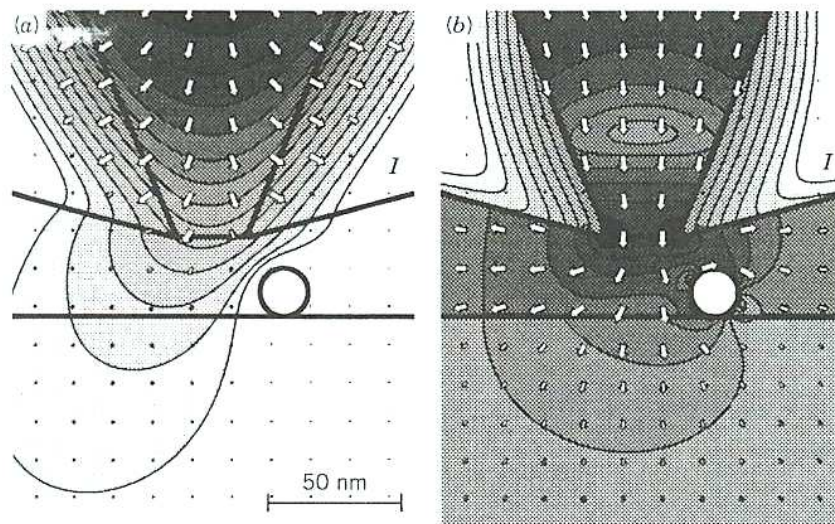
Figure 79: Calculated intensity in the near-field of an aperture above a perfectly conducting cylinder (multiple-multipole-method). [from Paesler, Moyer "Near-Field Optics"]

Another example (figure 80) shows the signal when scanning across two dielectric stripes for three different distances between the stripes. The calculations are numerical solutions of Maxwell's equations via the *Finite-Difference-Time-Domain, FDTD method.*
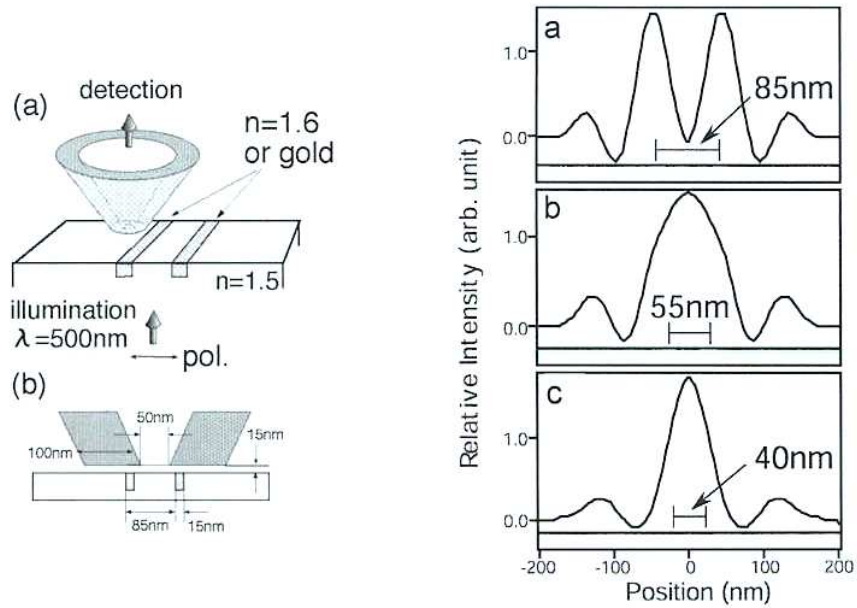
Figure 80: Signal when scanning across two dielectric stripes (calculated by the FDTD method). [from Kawata, Ohtsu, Irie "Nano-Optics"]

An additional complication of SNOM imaging results from the pronounced polarization dependence. As an example the SNOM signal of a probe which is scanned across a metallic step is shown in figure 81.
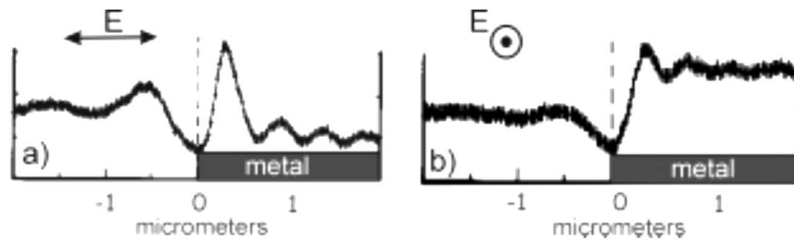
Figure 81: Measured signal of SNOM probe scanned across a metallic step for two different polarizations [from Huser, J. Opt. Soc. Am. A 16, 141 (1999)]

4.2 SNOM Concepts

There are three basic points regarding the difficulties of SNOM:

1. Realization of a sub-wavelength scatterer

2. Scanning of an object with the scatterer

3. Detection of a tiny signal (possibly against a large background)

There are the following approaches to solve the problems:

1. Fabrication of tiny SNOM tips. At first pulled glass pipettes were used and later replaced by pulled and/or tapered optical fibers. Details are introduced below.

2. Invention of methods to control the distance between tip and object. Here methods from scanning tunneling and sacnning force microscopy were applied. Details below.

3. Partially, a solution is to use probes with sub-wavelength dimension, but at the same time high transmission. Filtering and lock-in techniques are applied as well..

The following figure 82 shows different SNOM concepts:
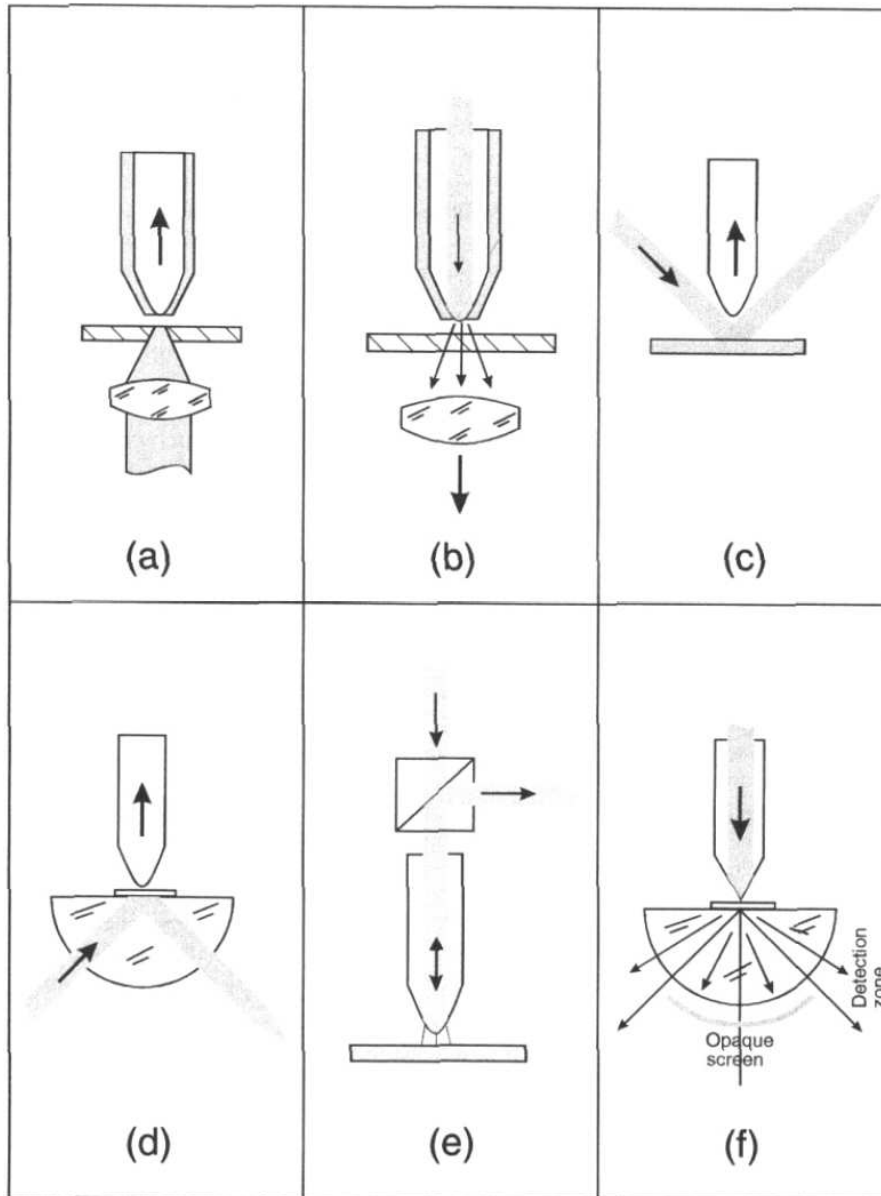
Figure 82: Different SNOM concepts. [from Courjon, Bainier, Rep. Prog. Phys. 57, 989 (1994)]

a) Transmission/collection mode: The tip is coated with metal except a small opening, i.e., the aperture.

b) Transmission/illumination mode: The tip acts as a "nano light source"

c) External reflection/collection mode: The tip collects locally scattered fields from the object.

d) Internal reflection/collection mode: Photon Scanning Tunneling Microscopy, PSTM or Scanning Tunneling Optical Microscopy, STOM)

e) External illumination/collection mode: combination of a) and b)

f) Internal reflection/illumination mode: Inverted Photon Scanning Tunneling Microscopy (PSTM)

Advantages or disadvantages of the different possible configurations have to be judged with respect to the desired applications, i.e., taking into account the criteria: simplicity of the setup, background reduction, sensitivity, resolution, etc.

There are three modi of scanning the probe across the object (see figure 83:

1. Constant Height Modus

2. Constant Intensity Modus

3. Constant Distance Modus
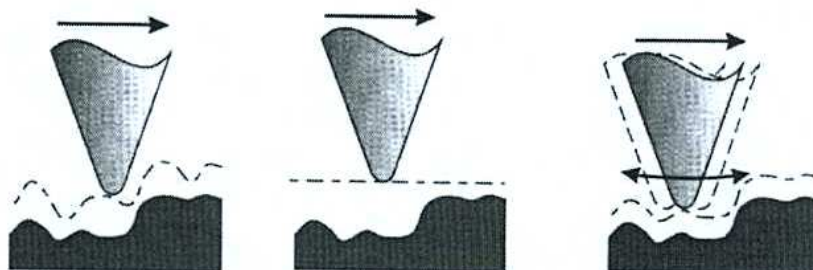
Figure 83: Constant intensity (left), constant height (middle) and constant distance (right) modus in SNOM [from Courjon, Bainier, Rep. Prog. Phys. 57, 989 (1994)]

The Constant Height Modus and the Constant Intensity Modus provide the same image information!

If there is a z-dependence of the intensity (e.g. in Photon Tunneling Microscopy) then the measured mean intensity provides a control signal to stabilize the distance between probe and object. It is straightforward to derive this statement if the following geometry (figure 84) is assumed:
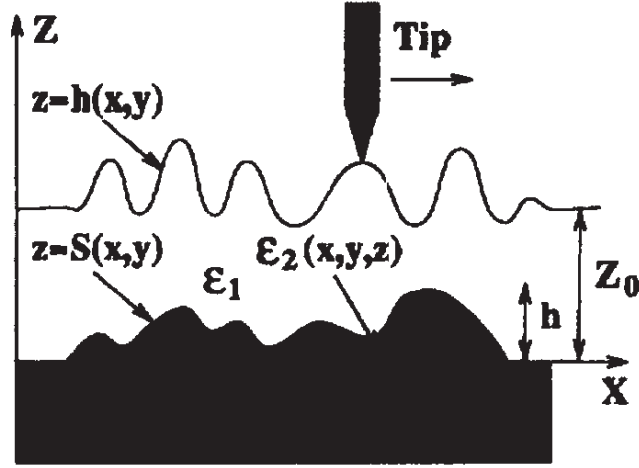
Figure 84: Geometry in constant height and constant intensity mode. [from Greffet, Carminati, Prog. Surf. Sci. 56, 133 (1997)]

The optical signal is

$$S(r_{||}, z) = S^0(z) + S^1(r_{||}, z) \tag{243}$$

where the fraction $S^0(z)$ results from a flat substrate and $S^1(r_{||}, z)$ from the object. If one follows a flat surface in constant intensity mode it is

$$h(r_{||}) = z_0 + \delta h(r_{||}) \tag{244}$$

where $z_0 = \langle h(r_{||}) \rangle$. Along $h(r_{||})$ it is

$$S^0(h(r_{||})) + S^1(r_{||}, h(r_{||})) = S^0(z_0) \tag{245}$$

A first order expansion at $z = z_0$ results in:

$$\frac{dS^0}{dz}(z_0)\delta h(r_{||}) + S^1(r_{||}, z_0) + \frac{dS^1}{dz}(r_{||}, z_0)\delta h(r_{||}) = 0 \tag{246}$$

115

The last term can be neglected compared to the first two (if the decay length of the relevant evanescent fields is significantly larger than the variation δh). Then, it follows

$$h(r_{||}) = \frac{-S^1(r_{||}, z_0)}{\frac{dS^0}{dz}(z_0)} + z_0 \tag{247}$$

This means that the surface of constant intensity is proportional to the signal $S^1(r_{||}, z_0)$ obtained at constance distance z_0.

The following figures 85 and 86 illustrate two scenarios and numerical simulation of a near-field measurement in collection mode, respectively.
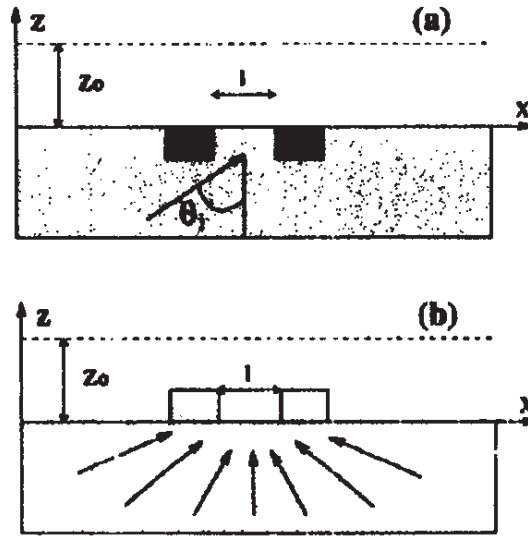
Figure 85: Numerical simulation: (a) two gold particle with w=$\lambda/10$, $h = \lambda/40$ in glass with $l = \lambda/8$; (b) glass substrate with w=$\lambda/4$, $h = \lambda/40$ und $l = \lambda/10$ [from Greffet, Carminati, Prog. Surf. Sci. 56, 133 (1997)]
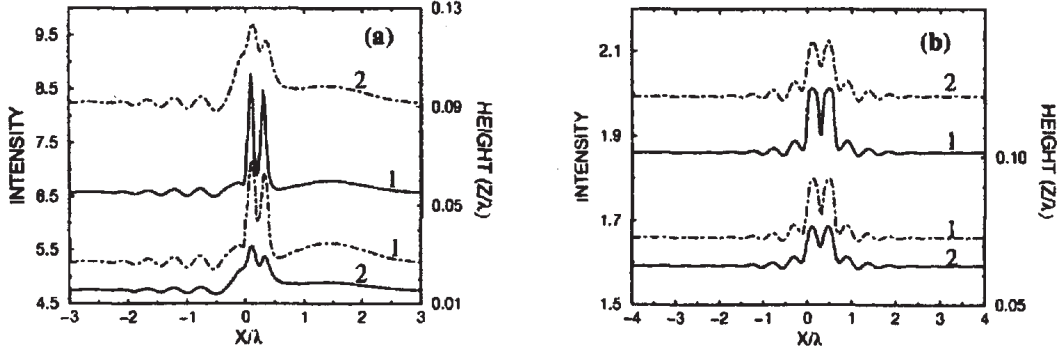
Figure 86: (a) Corresponding to fig. 85 (a). Constant intensity curves (dashed) and constant height curves (solid) for two different distances $z_0 = 0.03\lambda$ (curves 1) and $z_0 = 0.09\lambda$ (curves 2); (b) Corresponding to fig. 85 (b) with $z_0 = 0.07\lambda$ (curves 1) and $z_0 = 0.12\lambda$ (curves 2). [from Greffet, Carminati, Prog. Surf. Sci. 56, 133 (1997)]

In constant distance mode a SNOM probe is scanned in constant distance across an object. The control signal allowing distance control (discussed below) thus simultaneously provides information about the **topography**.

*In general there is a coupling between topography and optical near-field signal in constant distance mode! These **artifacts** are a especially problematic.*

We assume the geometry of figure 87:

In constant distance mode the SNOM tip follows the path

$$z = f(r_{||}) = z_0 + \delta f(r) \quad \text{mit} \quad z_0 = \langle f(r_{||}) \rangle \tag{248}$$

Then, the optical signal is

$$S(r_{||}, z = f(r_{||})) = S^0(f(r_{||})) + S^1(r_{||}, f(r_{||})) \tag{249}$$

Similar as shown above, a first order expansion around $z = z_0$ results in:

$$S(r_{||}, z = f(r_{||})) = S^0(z_0) + \frac{dS^0}{dz}(z_0)\delta f(r_{||}) + S^1(r_{||}, z_0) \tag{250}$$

The second term follows the topography of the object $\delta f(r_{||})$ and is unrelated to the optical near-field information. If this part is dominating then the information is
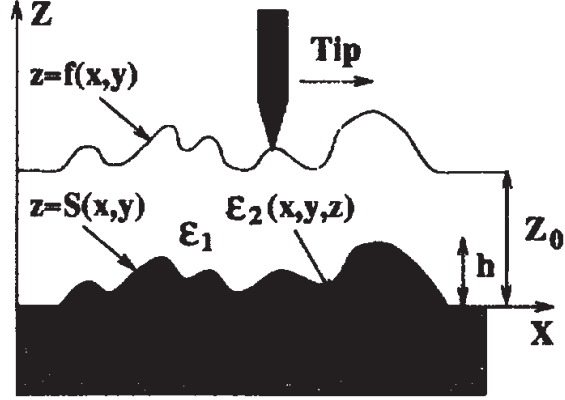
Figure 87: Geometry in constant distance mode. [from Greffet, Carminati, Prog. Surf. Sci. 56, 133 (1997)]

the same as in an atomic force microscope (AFM) with an optical read-out of the tip-sample distance! The parameter Γ

$$\Gamma = \frac{dS^0}{dz}(z_0)/S^1(r_{||}, z_0) \tag{251}$$

determines the size of this **artifact**. The following numerical simulations demonstrate the effect of artifacts. In the first figure 88 illumination is performed with a plane wave under normal incidence, i.e., $\frac{dS^0}{dz}(z_0) = 0$. Therefore, constant height and constant distance mode provide the same results.

In the next figure 89 the illumination is again via a plane wave, but under an incidence angle of $60°$, i.e., $\frac{dS^0}{dz}(z_0) \neq 0$. The difference of constant height and constant distance mode is an artifact caused by the sample's topography.

118

transmission, θ$_i$=0°, s-polarization
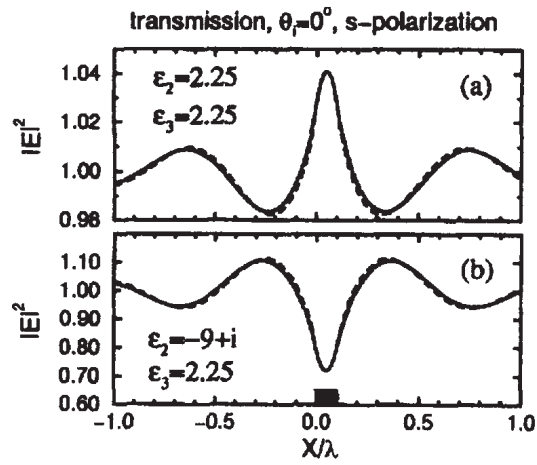
Figure 88: Calculated near-field signal above a bar of width $w = 0.1\lambda$ and height $h = 0.015\lambda$ for two different ε and illumination under normal incidence. Solid: constant height mode with $d = 0.0225\lambda$; Dashed: constant distance mode with $d = 0.0075\lambda$. [from Greffet, Carminati, Prog. Surf. Sci. 56, 133 (1997)]

TIR, θ$_i$=60°, s-polarization
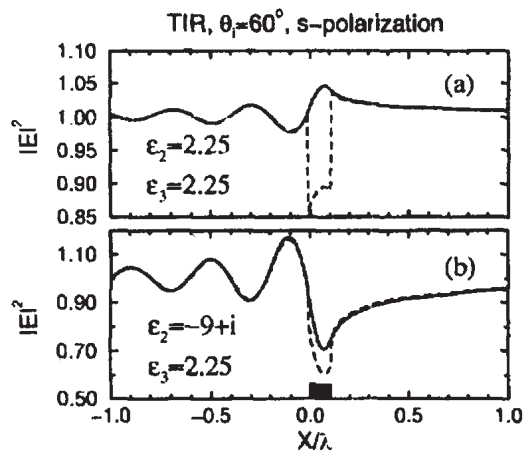
Figure 89: Same as above, but with illumination under an incidence angle of 60°. Solid: Constant height mode with $d = 0.0225\lambda$; Dashed: Constant distance mode with $d = 0.0075\lambda$. [from Greffet, Carminati, Prog. Surf. Sci. 56, 133 (1997)]

119

Artifacts in SNOM images may give the wrong impression of enhanced optical resolution, as shown in the following example (figure 90):
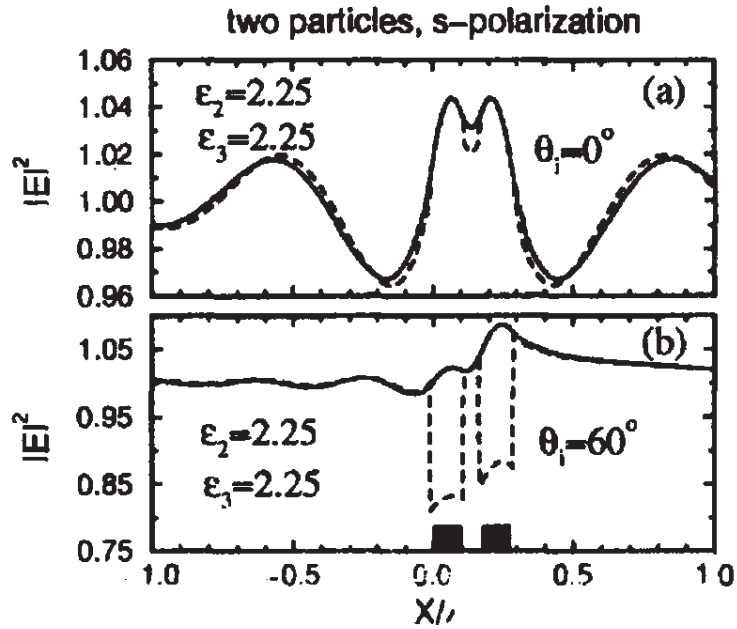
Figure 90: Calculated near-field signal above two bars of width $w = 0.1\lambda$, height $h = 0.015\lambda$ and distance $l = 0.075\lambda$ for two different ε at $0°$ and $60°$ angle of incidence of illumination. Solid: Constant height mode with $d = 0.0225\lambda$; Dashed: Constant distance mode with $d = 0.0075\lambda$. [from Greffet, Carminati, Prog. Surf. Sci. 56, 133 (1997)]

4.3 Experimental Realizations

The following figure 91 shows a typical SNOM setup.
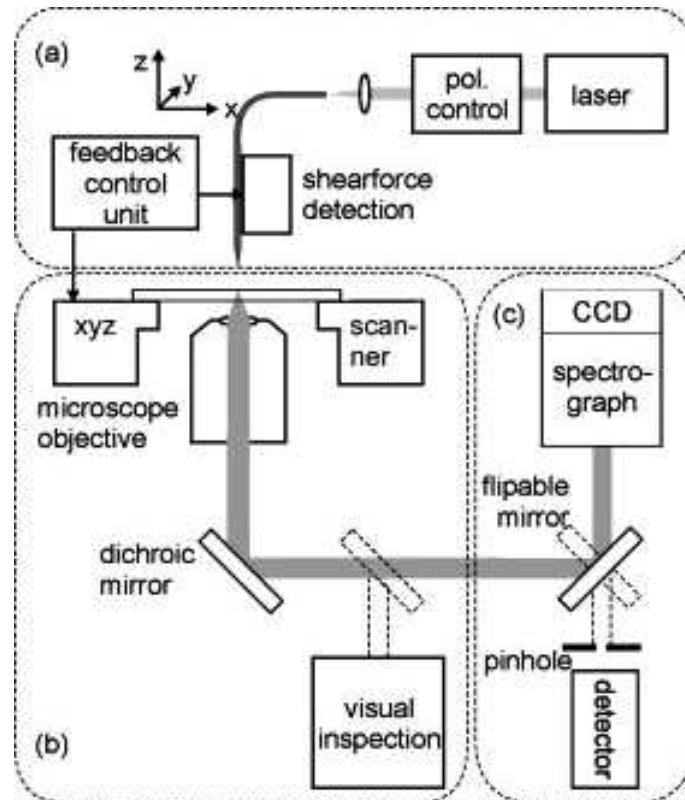
Figure 91: A typical SNMO setup in illuminarion/collection mode [from Hecht et al., J. Chem. Phys., 112, pp. 7761-7774 (2000)].

A technical difficulty of SNOM and other scanning-probe techniques such as scanning Tunneling Microscopy (STM) or Atomic Force Microscopy (AFM) is scanning of a probe at a nearly constant distance of few nm across a sample. In order to do that a **Feedback-Signal** is required.

The following figure 92 summarizes different approaches for feed-back control.
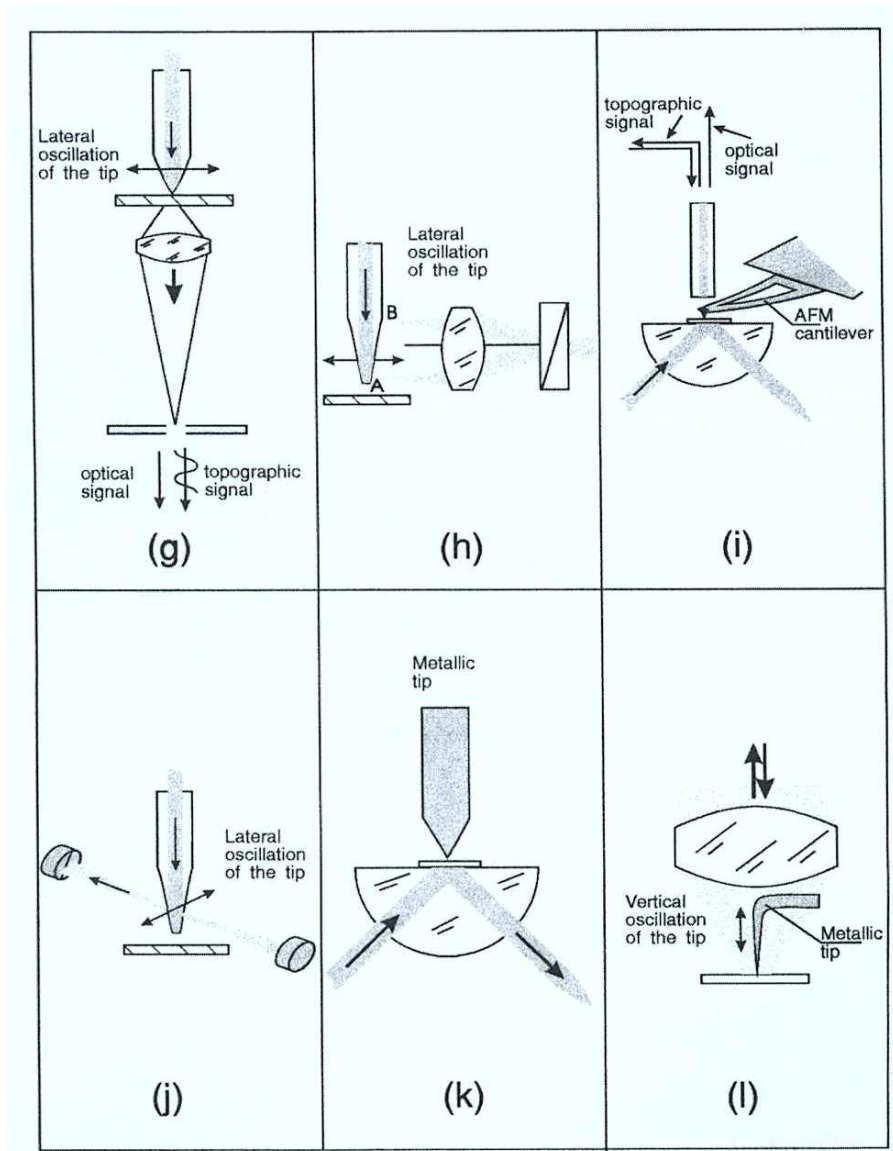
Figure 92: Different configurations in near-field microscopy. [from Courjon, Bainier, Rep. Prog. Phys. 57, 989 (1994)]

g) Shear-force method: Light from the tip is imaged on a pinhole. The constant part of the signal corresponds to the near-field signal, the strongly modulated part is used for feed-back control.

h) As in g), but with a detection of the tip oscillation from the side via two focussed lasers.

i) AFM (in contact-mode) with a hollow tip as SNOM probe.

j) Detection of the tip oscillation via a laser and a quadrant detector.

k) Internal reflection perturbation method with an opaque tip.

l) External reflection perturbation method with an opaque tip.

- In Constant-Intensity-Mode the feed-back signal is derived directly from the detected intensity. In this case the signal does not contain any topographic information. If there are strong height gradients on the sample, there is a significant risk of "crashing" and thus destroying the tip.

- The most flexible method is the shear-force method in constant-distance mode which will be discussed in the following.

In the **shear-force method** an oscillation of the tip is excited (oscillation frequency 10 to 150 kHz, see figure 93). When the tip approaches a surface, the oscillation amplitude, phase, and resonance frequency of the tip changes (see figure 94). This can be utilized to stabilize the tip-surface distance to approximately 5-10 nm. The shear-force results from different interactions of the tip with the surface, such as adhesion, van-der-Waals force, Coulomb interaction, etc. As the shear-force depends also on the tip, there is no simple correspondence of the detected and the real topography.
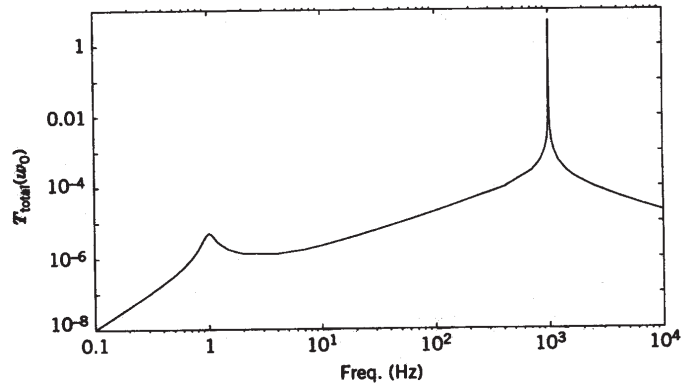
Figure 93: Resonance curve of a SNOM probe on an optical table. 1 Hz corresponds to the resonace of the table, 1 kHz to the resonace of the SNOM tip. [from Paesler, Moyer "Near-Field-Optics"]
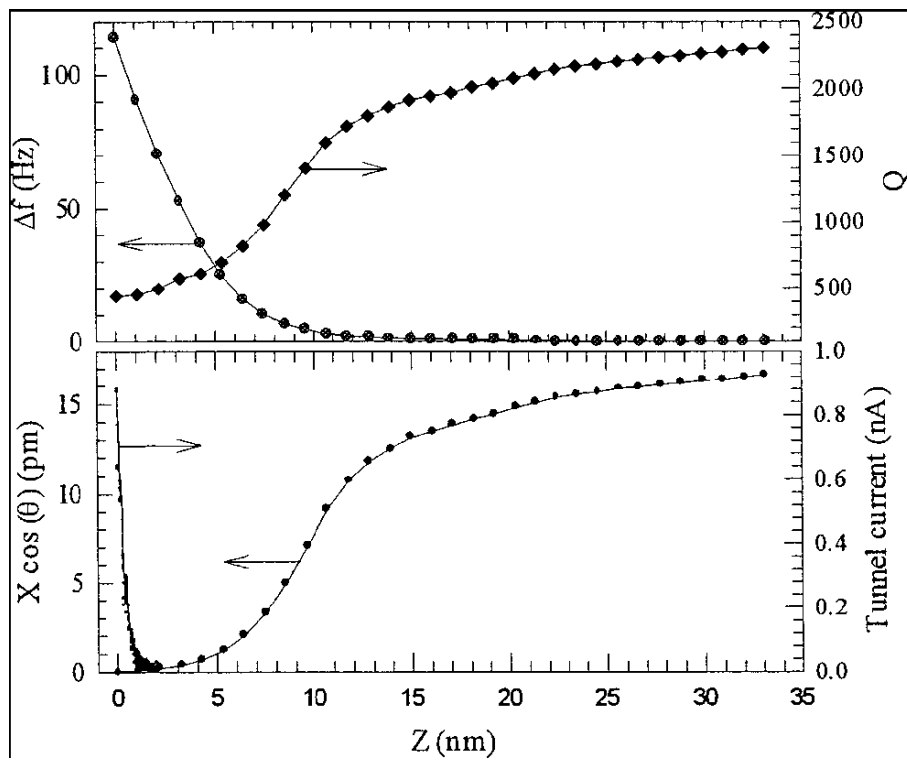
Figure 94: Change of resonance frequency, quality factor, and tunnel current of a metal coated tip during approach [Grober et al., Rev. Sci. Instr. 71, 2776 (2000)]

124

The detection of oscillation can de done optically or electronically. In order to excite oscillation of the tip it can be excited via a four-segmented piezo tube or a commercial piezo tuning fork (see figure 94 and 96, respectively).
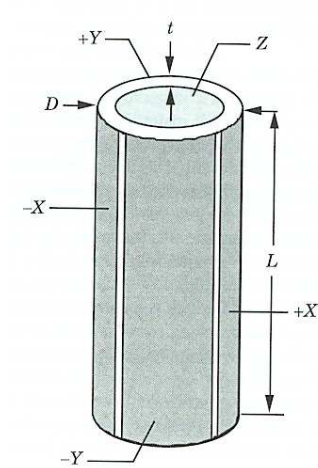
Figure 95: A four-segmented piezo tube. A SNOM tip is glued inside the tube. [from Paesler, Moyer "Near-Field-Optics"]
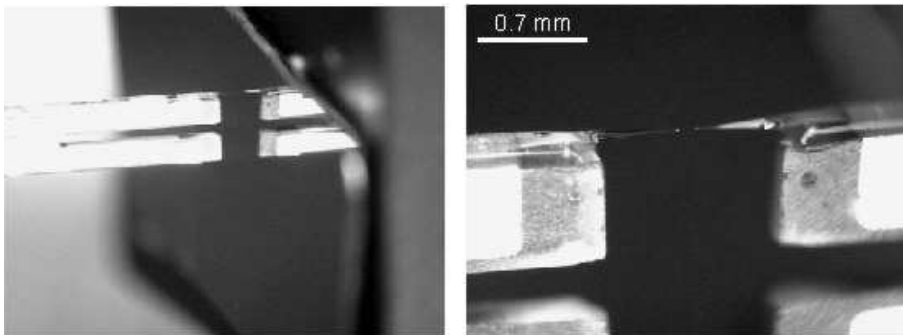
Figure 96: SNOM tip on a tuning fork.

A further challenge in SNOM is the **fabrication of SNOM tips**. A typical aperture SNOM tip consists of a metal-coated tapered glass fiber with a very small opening. Key feature is a small opening, but a large transmission at the same time.

First SNOM experiments were performed with pulled metal-coated micro-pipettes. They have a well defined aperture shape, but poor transmission.

The following figures show metal-coating and transmission through a fiber:
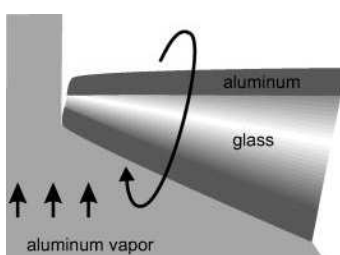
Figure 97: Schematics of metal-coating a SNOM tip [from Hecht et al., J. Chem. Phys., 112, pp. 7761-7774 (2000)]
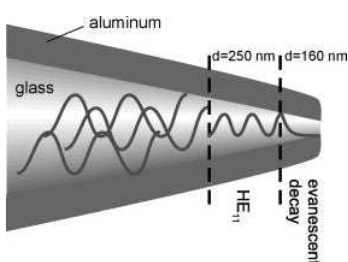
Figure 98: Schematics of light transmission through an aperture probe [from Hecht et al., J. Chem. Phys., 112, pp. 7761-7774 (2000)]
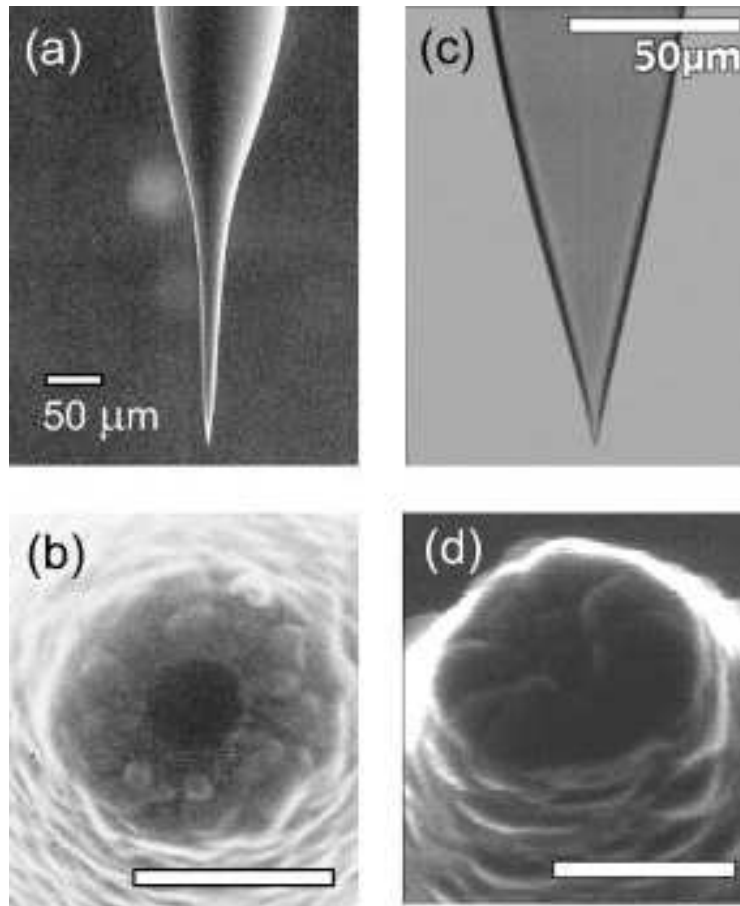
Figure 99: Optical (b) and SEM (a, c, d) pictures of pulled (left column) and etched (right column) SNOM tips. Scale bar = 300 nm. [from Hecht et al., J. Chem. Phys., 112, pp. 7761-7774 (2000)]

Another method to obtain tips with a small diameter (below 100 nm) is chemical etching. The following schematics illustrate the Turner method and tube etching.
In Turner etching the glass tips are dipped in hydrofluric (HF) acid which is coveerd with a thin film of an organic liquid. Etching is self-terminating.
In tube etching the polymer coating of a commercial fiber is not stripped-off. Therefore, etching occurs within a tiny tube, i.e., within a well protected and defined environment and is thus well reproducible.
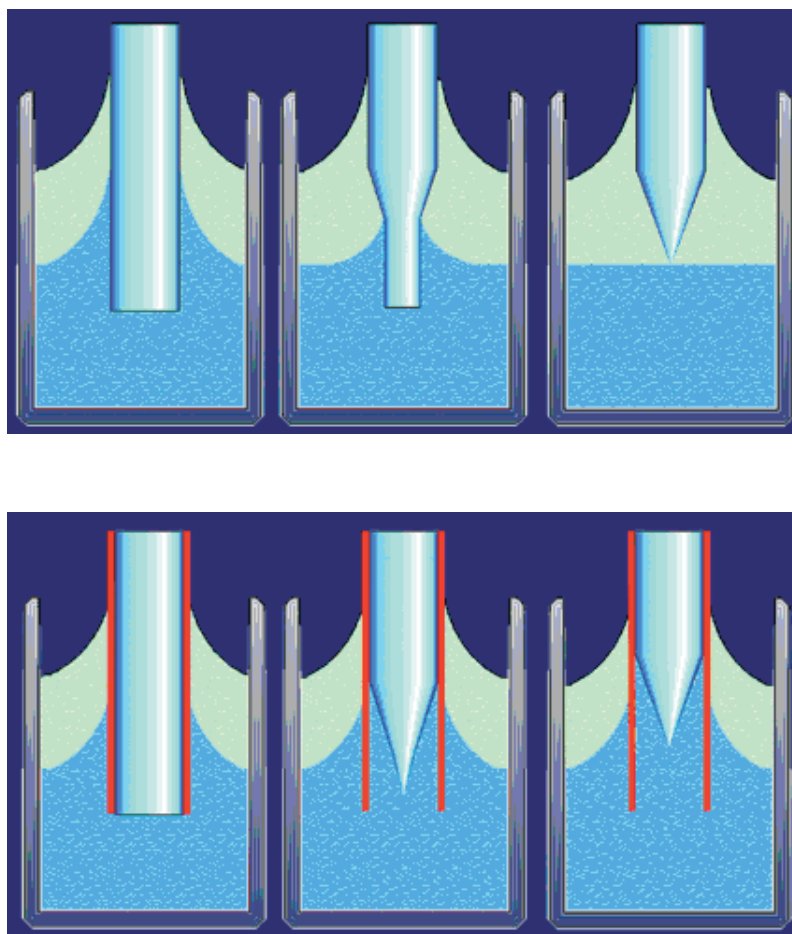
Figure 100: Turner etching (top) and tube-Etching (bottom).
[from http://www.ceac.ethz.ch/zenobi/research/nanoscale/tip/overview.html]

The following figures illustrate various tips as examples.
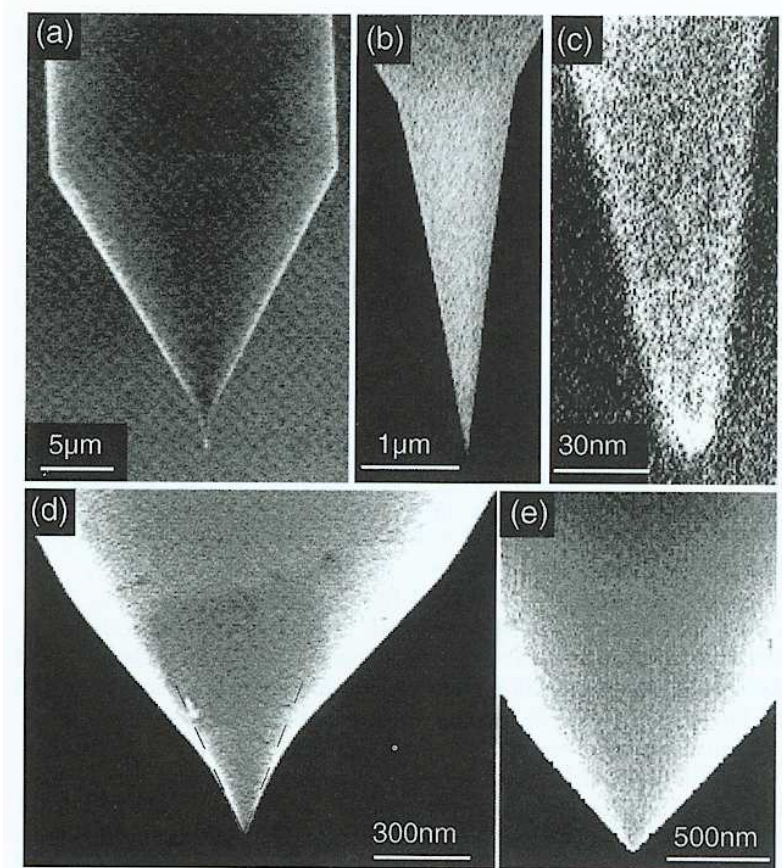
Figure 101: SEM-images of various etched fiber tips. [from Ohtsu, "Near-Field Nano/Atom Optics"]

With high-throughput tips it is possible to obtain transmissions of 10^{-3} to 10^{-2} while the aperture diameter is below 80 nm. The following figure 102 shows the relation between measured transmission and aperture diameter for different tips.
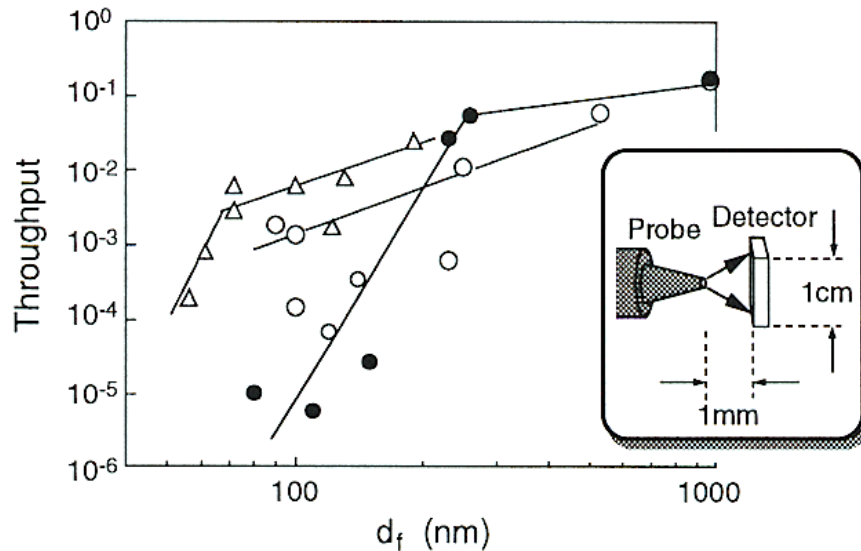
Figure 102: Measured transmission of different SNOM tips. Filled circles; conventional tips, open circles and triangles: high-throughput tips [from Ohtsu, "Near-Field Nano/Atom Optics"]

Similar as in Scanning Confocal Optical Microscopy, SCOM, the image in SNOM is obtained point-wise. A **scanning** of the probe is required.

Typically, the SNOM probe is at a fixed position while the sample is scanned for the following reasons:

- Optical methods to detect the oscillation of the tip require a fixed tip position.

- The detection optic can be at a fixed position, which is particularly advantageous when detecting the SNOM signal confocally (with reduced background).

- The signal can be coupled into an optical fiber, which is required e.g. in low-temperature SNOM setups within a cryostat.

As scanners commercial piezoelectric stages or tube scanners are used. The following figures show three different SNOM setups (SNOM in Internal Reflection Collection mode, SNOM in Transmission Illumination mode, low-temperature SNOM).
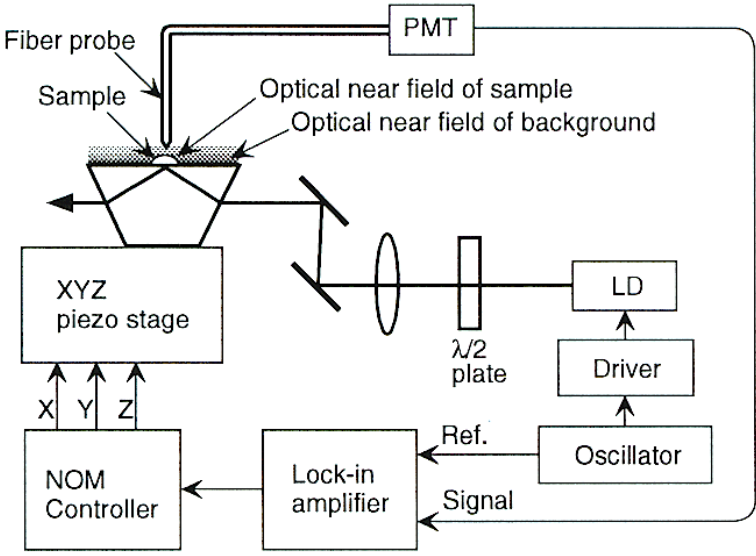
Figure 103: SNOM in Collection Mode [from Ohtsu, "Near-Field Nano/Atom Optics"]
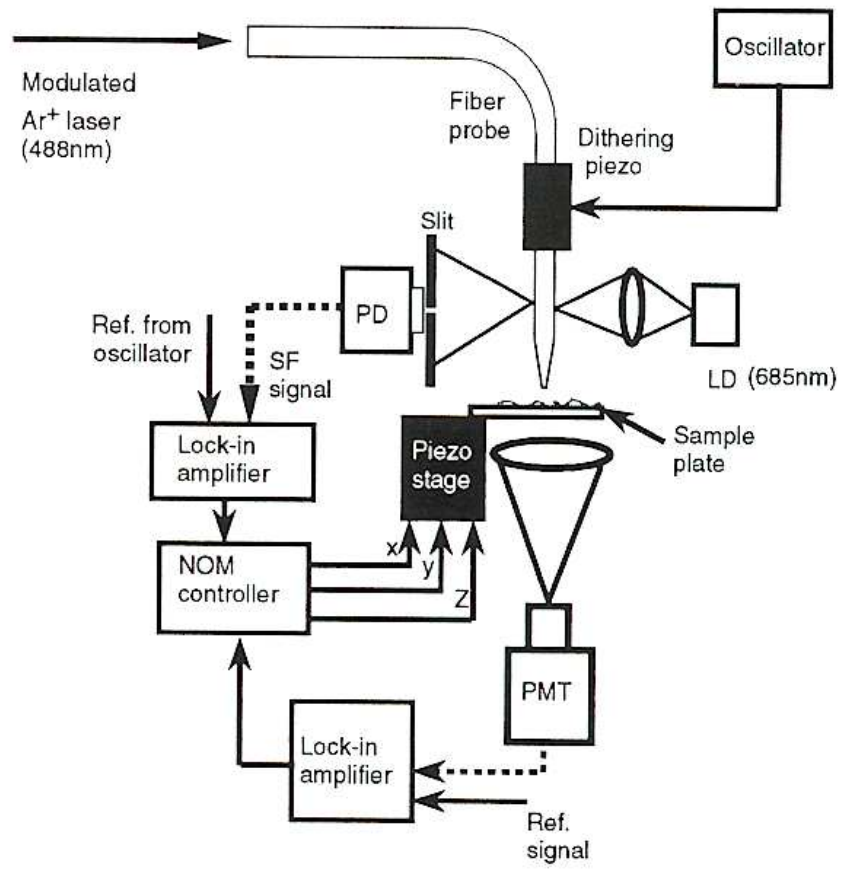
Figure 104: SNOM in Illumination Mode [from Ohtsu, "Near-Field Nano/Atom Optics"]
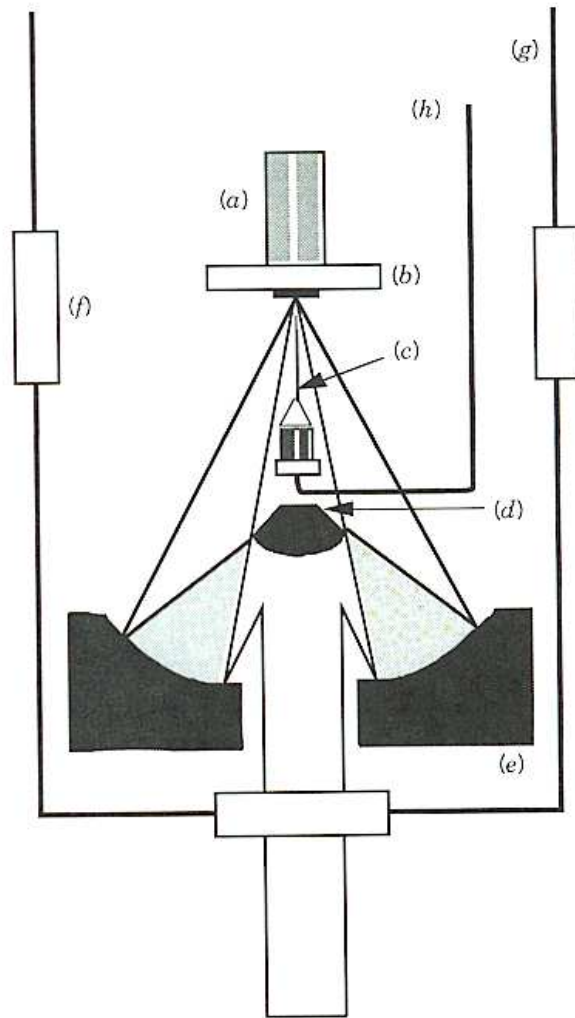
Figure 105: Low-temperature SNOM in a cryostat; (a): Piezo-tube scanner, (b):Sample, (c): SNOM tip, (d): illumination mirror, (e): parabolic mirror, (f): window, (g): cryostat, (h): optical fiber [from Paesler, Moyer "Near-Field-Optics"]

4.4 SNOM Theory

A simple model
Paesler und Moyer [Paesler/Moyer, "Near-Field Optics"] consider a simple model (figure 106) to analyze the microscopy in the far- and near-field:
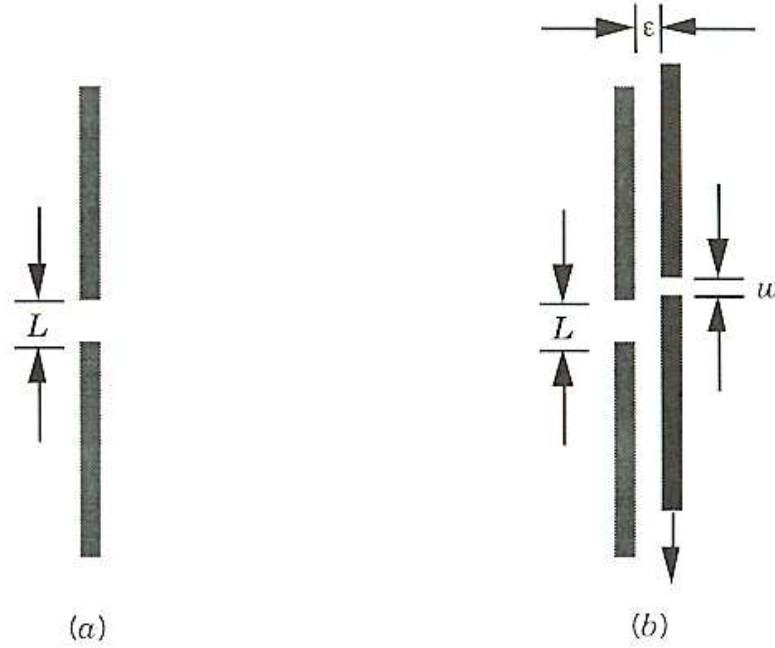
Figure 106: Model for microscopy in the far-field (a) and near-field (b) [from Paesler/Moyer, "Near-Field Optics"]

In the theory chapter we used the plane-wave expansion method to express the field $f(x, z = Z)$ via its Fourier components $F(\alpha, z = 0)$ at $z = 0$ as follows:

$$f(x, z = Z) = \int\limits_{-\infty}^{\infty} d\alpha_x \exp(-2\pi i \alpha_x x) F(\alpha, z = 0) \exp(-2\pi i(\alpha^2 - \alpha_x^2)^{1/2} Z) \quad (252)$$

In the far-field only the following components contribute

$$(\alpha^2 - \alpha_x^2) < 0 \quad (253)$$

i.e. evanescent fields can be neglected. If we assume (see figure 106) for the field at $z = 0$

$$f(x, z = 0) = E_0 \ rect(x/L) \quad (254)$$

134

it follows for the far-field in case (a):

$$f(x, z = Z) = \int\limits_{-\omega/2\pi c}^{\omega/2\pi c} d\alpha_x \exp(-2\pi i \alpha_x x)\frac{\sin \alpha_x L}{\alpha_x} \exp(-2\pi i (\alpha^2 - \alpha_x^2)^{1/2} Z) \quad (255)$$

In case of an additional aperture (b) at a distance $z = \epsilon$ it is

$$f(x, z = \epsilon) \quad = \quad E_0(x, z = \epsilon)\, rect(x/w) \quad\quad (256)$$

$$E_0(x, z = \epsilon) \quad = \quad \int\limits_{-\infty}^{\infty} d\alpha_x \exp(-2\pi i \alpha_x x) F(\alpha_x, z = 0) \exp(-2\pi i (\alpha^2 - \alpha_x^2)^{1/2}\epsilon)$$

for the far field

$$f(x, z = Z) = \int\limits_{-\omega/2\pi c}^{\omega/2\pi c} d\alpha_x \exp(-2\pi i \alpha_x x) \exp[-2\pi i (\alpha^2 - \alpha_x^2)^{1/2}(Z - \epsilon)] \quad (257)$$

$$\times \int\limits_{-\infty}^{\infty} d\alpha_x' \exp(-2\pi i \alpha_x' x) F(\alpha_x', z = 0)\frac{\sin(\alpha_x - \alpha_x')w}{(\alpha_x - \alpha_x')} \exp[-2\pi i (\alpha^2 - \alpha_x'^2)^{1/2}\epsilon]$$

If we now consider for simplicity only one far-field component ($F(\alpha_x, z = 0) = \delta(\alpha_x - K)$) it follows for the case (a):

$$f(x, z = Z) \quad = \quad E_0 \exp(-2\pi i K x) \exp[-2\pi i (\alpha^2 - K^2)^{1/2} Z] \quad \text{if } K < \omega/c$$
$$= \quad 0 \quad \text{if } K > \omega/c \quad\quad (258)$$

and for the case (b):

$$f(x, z = Z) = E_0 \exp[-2\pi i (\alpha^2 - K^2)^{1/2}\epsilon] \quad\quad (259)$$

$$\times \int\limits_{-\omega/2\pi c}^{\omega/2\pi c} d\alpha_x \exp(-2\pi i \alpha_x x) \exp[-2\pi i (\alpha^2 - \alpha_x^2)^{1/2}(Z - \epsilon)]\frac{\sin(\alpha_x - K)w}{\alpha_x - K}$$

In the limit $w \to \infty$

$$\frac{\sin(\alpha_x - K)w}{\alpha_x - K} \to \delta(\alpha_x - K) \quad\quad (260)$$

both cases are identical.

135

It is apparent that the far-field contains higher spatial frequencies only in case (b).

This simple model can be applied to a more relevant case (detection of a double-slit) as shown in figure 107: It is possible to find rather simple integral expressions for
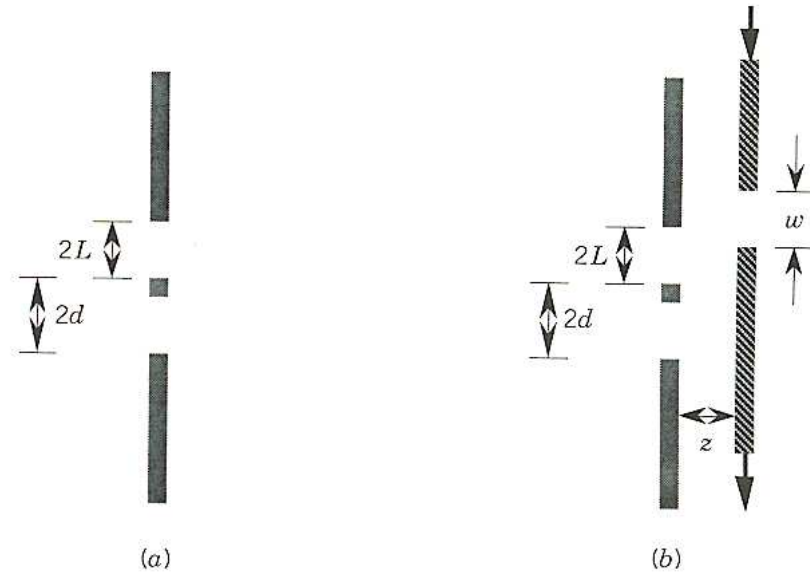
Figure 107: Model to study optical resolution with far-field (a) and near-field (b) microscopy. [from Paesler/Moyer, "Near-Field Optics"]

the cases (a) and (b) which we will not provide here. Instead the results are plotted in the following figure 108:
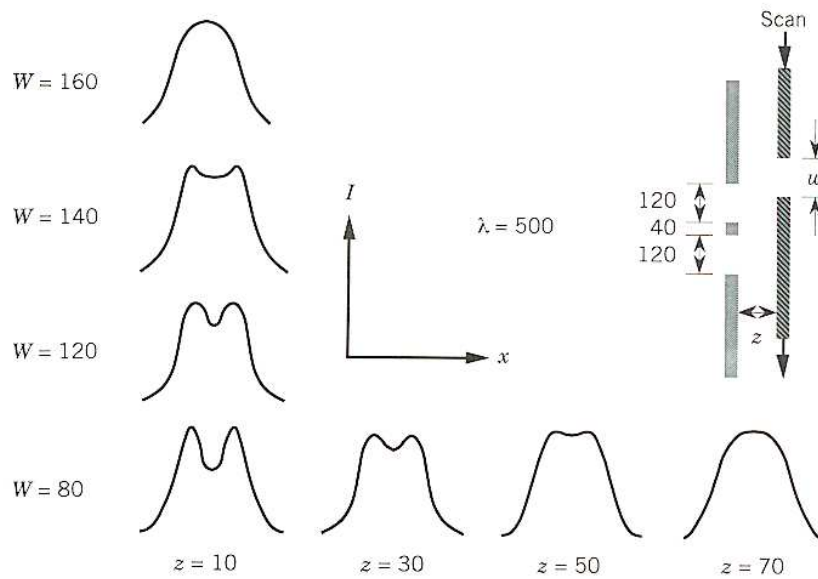
Figure 108: Calculated images of a double-slit in the near-field for different dimensions of the aperture and different distances z of the aperture from the slit. [from Paesler/Moyer, "Near-Field Optics"]

For quantitative modeling of near-field problems numerical simulations are required. These can rely on different approaches such as:

Multiple-Multipole-Method (MMP Method)
see for example: C. Hafner, *The generalized Multipole Technique for Computational Electromagnetics*, Boston, MA, ARTECH House 1990.

Finite Difference Time Domain (FDTD)
which is a purely numerical method. See for example: A. Taflove und K. R. Umanshankar, *The Finite Difference Time Domain Technique*, Amsterdam, Elsevier 1990.

Volume-Integral-Methode

This methods starts form the volume-integral equations as discussed in the theory chapter:

$$E(r) = E^0(r) + \int_{sample} [\varepsilon_{sample}(r') - \varepsilon] \overleftrightarrow{G}(r_{\parallel} - r'_{\parallel}, z, z') E(r') \, dr' \qquad (261)$$

$E(r)$ is the field distribution resulting from an illuminated sample via integration over the sample volume. Here, ε_{sample} is the dielectric constant of the sample and E^0, $\overleftrightarrow{G}$ are the (possibly analytically) known field, and Green's function for a plain substrate without the sample. A first order approximation (Born-approximation $E(r') = E^0(r')$) often provides sufficiently exact results. For details see for example Greffet und Carminati, Progr. Surf. Sci. **56**, 133 (1997).

4.5   SNOM Trends

In the previous section we basically discussed *aperture SNOM*. However, near-field microscopy relies on local scattering, which transfers non-propagating near-fields in propagating far-fields. In principle, local scattering can be realized without apertures.

Apertureless SNOM can be realized in different ways. The following figure 109 illustrates a local scattering process.
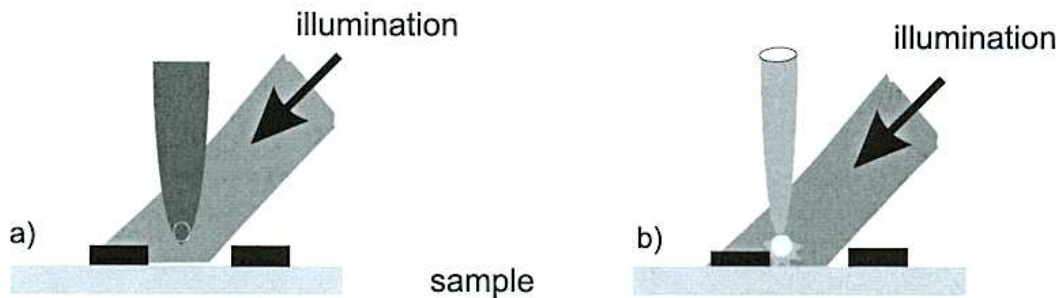
Figure 109: Schematics of apertureless SNOM: A scattering probe scatters near-fields locally at an object. [from V. Sandoghdar, "Trends and Developments in Scanning Near-field Microscopy"

A severe problem of apertureless SNOM is the detection of the scattering signal possibly against a large background. There are different techniques to divide the scattering signal (from scattered near-fields) from ordinary far-fields:

- Modulation: A small variation of the tip's position should only influence the local scattering process. Lock-in techniques are used to extract the scattering signal.

- Generation of a characteristic signal: A specific signal is generated which can only stem from the local scattering process, e.g.,
  a) local field enhancement and non-linear effects
  Close to a small scatterer (for example a tiny metal tip) boundary conditions often enforce a strong enhancement of local electric fields.
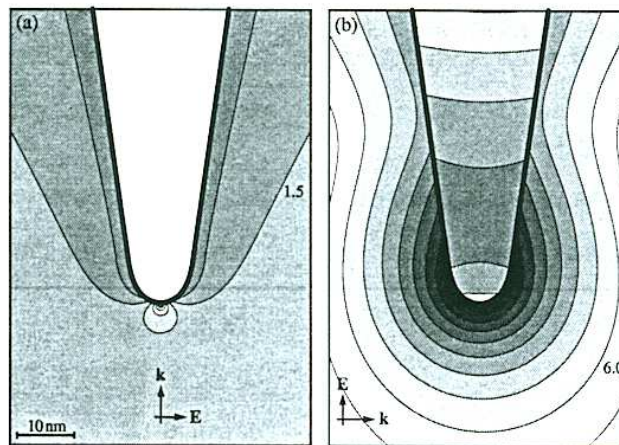
Figure 110: Local field enhancement at a gold tip (curvature radius 5 nm) for two different polarizations of the illumination.

The strong fields drive non-linear processes which produce a signal that is (spectrally) different from the background from the illumination source and can thus be easily detected. Examples are second harmonic generation (**SHG**) or surface enhanced Raman scattering (**SERS**).

139

b) Local plasmon resonances

The following figures show how a small gold particle (100 nm in diamanter) can be mounted on a SNOM tip. Its characteristic resonance frequency (plasmon resonance, as will be discussed in an later chapter) can be regarded as a tiny local light source.
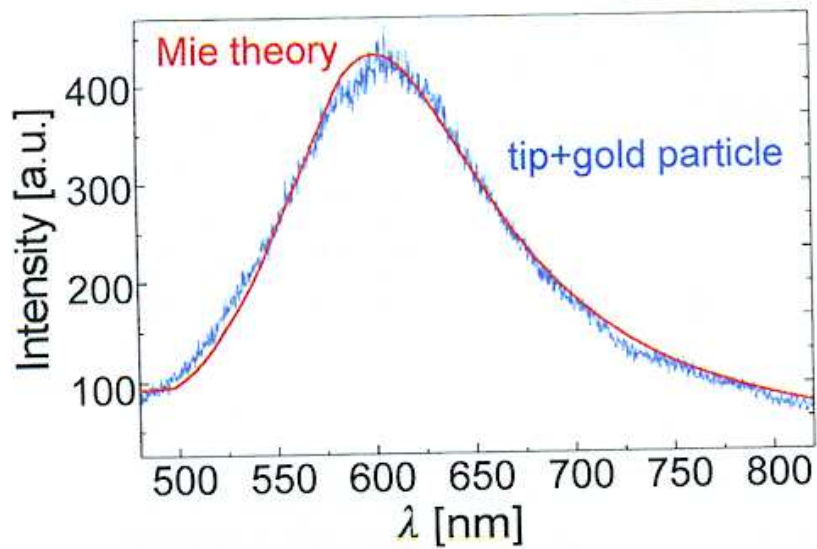
Figure 111: Measured and calculated plasmon resonance of a spherical gold particle at a SNOM tip. [from T. Kalkbrenner et al., J. Mic. 202, 72 (2000)]
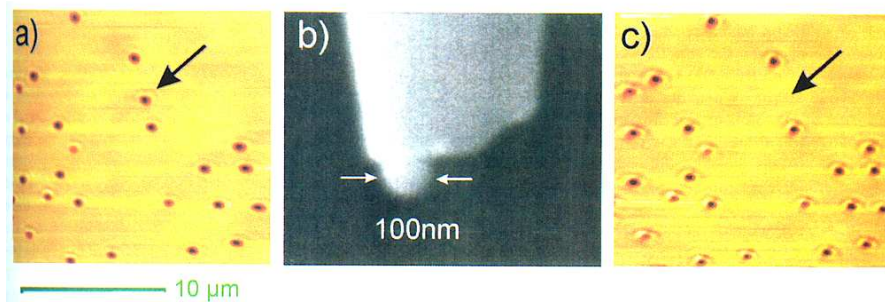
Figure 112: Attaching a gold particle to a SNOM tip. Middle: SEM image, Left and Right: microscope image. [from T. Kalkbrenner et al., J. Mic. 202, 72 (2000)]

c) Realization of a nanoscopic light source

An ultimate form of apertureless SNOM is the illumination of an object with a point-like source, e.g., a single molecule.
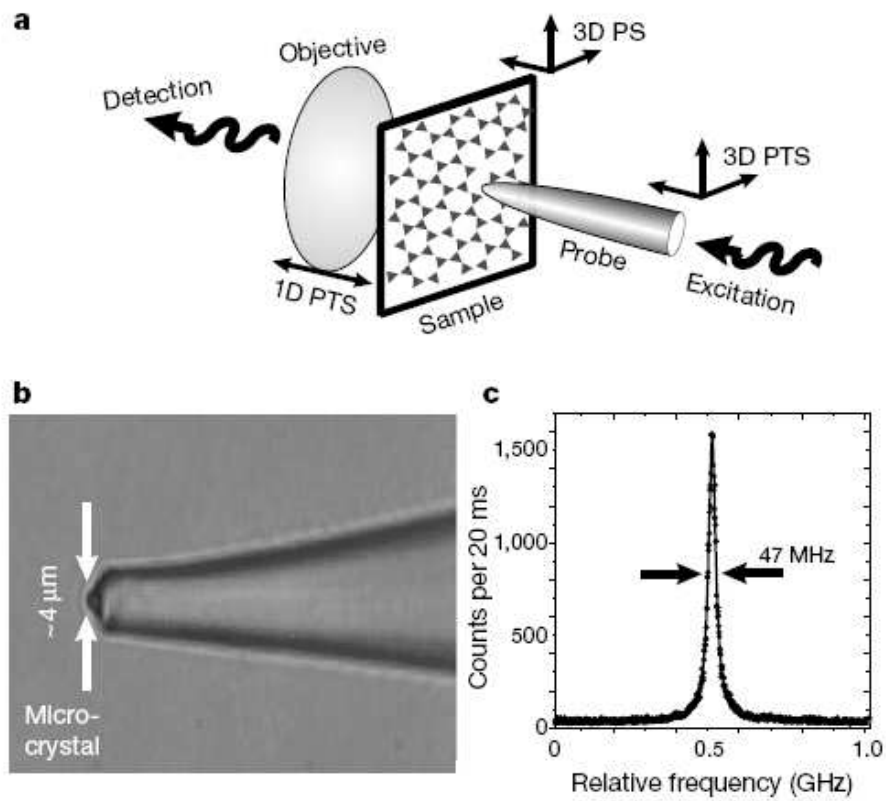
Figure 113: A single molecule as nanoscopic light source. a) Schematic view of the experimental configuration; b) an optical microscope image of the fibre probe displaying a micro-crystal of p-terphenyl glued to its end. The micro-crystal was lightly doped with terrylene molecules; c) An excitation spectrum of the molecule used for recording the images. [from Hettich et al., Nature 405, 325 (2000)]
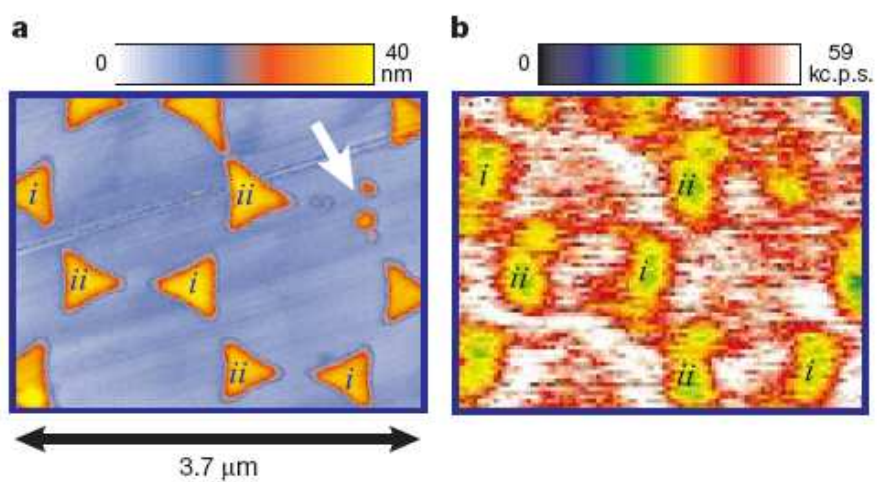
Figure 114: a) An atomic force microscope (AFM) topography image of the area of the sample; b) The optical raster-image recorded using the fluorescence of a single terrylene molecule for illumination. [from Hettich et al., Nature 405, 325 (2000)]

In the following, we provide some more trends in near-field optical microscopy:

- Reproducible fabrication of robust SNOM sensors using nanofabrication technology with the goal of **integration and parallelization** of SNOM.
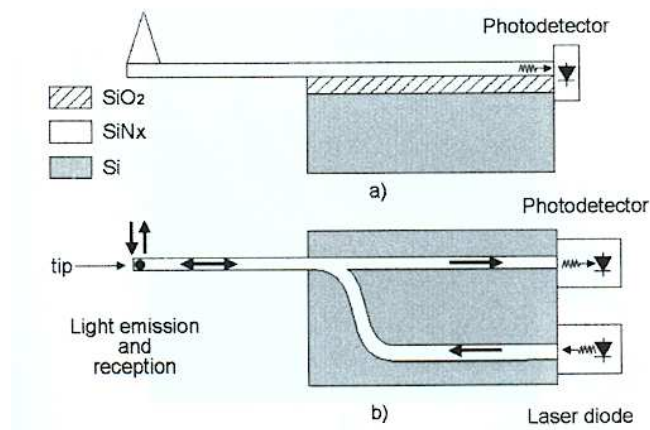
Figure 115: Design of an integrated structure consisting of a SNOM tip and a SiN-waveguide [from P. Gall-Borrut et al., J. Mic. 202, 72 (2000)]
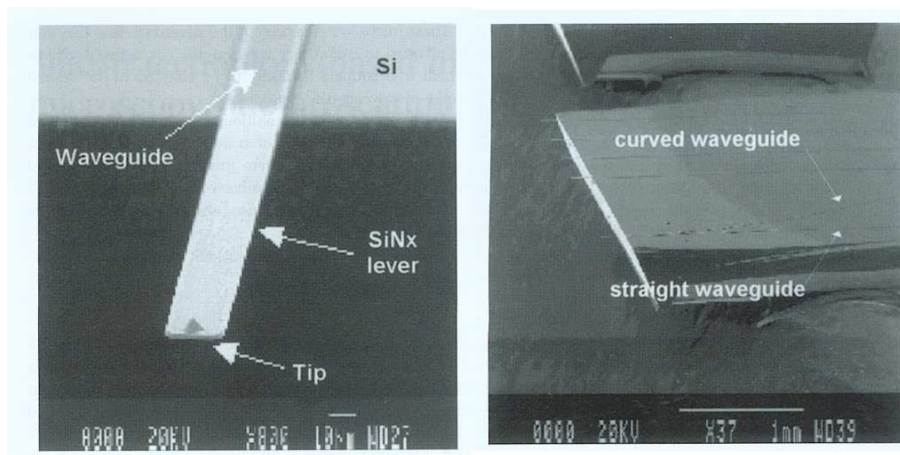
Figure 116: SEM image of one (left) and several (right) SiN SNOM cantilevers. [from P. Gall-Borrut et al., J. Mic. 202, 72 (2000)]

- Fabrication of **functionalized tips**, which provide an (optical) interaction only with specific probes. One example is the so-called fluorescence (Foerster) resonant energy transfer (**FRET**) where the optical excitation of a donor particles (attached to the tip) is transferred to specific acceptor particles (in the sample) which then fluoresce at a characteristic wavelength.
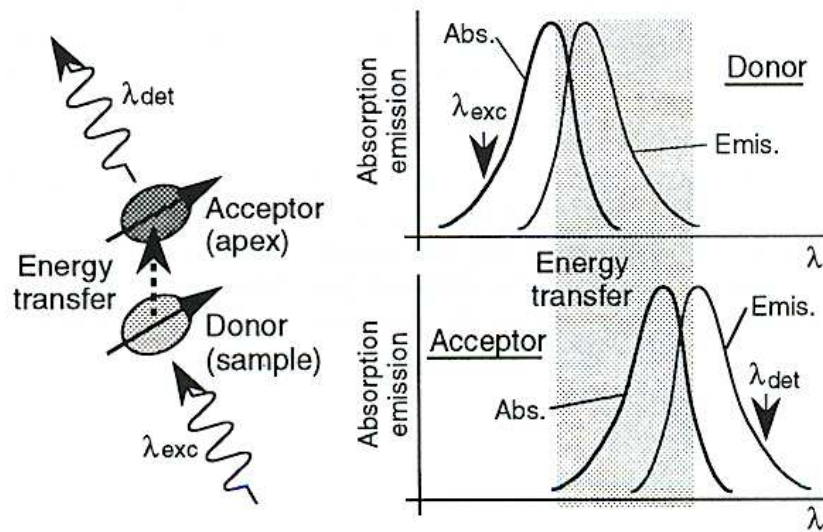
Figure 117: Schematics of Foerster Resonant Energy Transfer (FRET). [from Ohtsu, "Near-field Nano/Atom Optics and Technology"]
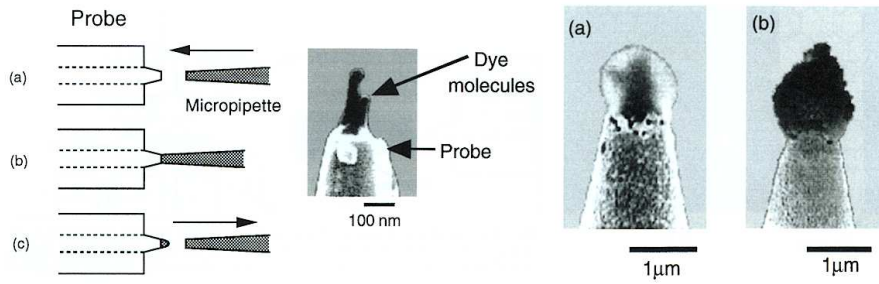
Figure 118: Fabrication of a functionalized SNOM probe (left), SEM-image of tips functionalized with PDA-Polymer (a) and GaAs powder (b). [from Ohtsu, "Near-field Nano/Atom Optics and Technology"]

- Optical **nano manipulation:** SNOM probes can be used to manipulate and eventually trap small particles. Even trapping of single atoms with the localized light at the end of a SNOM tip or an optical fiber was suggested.
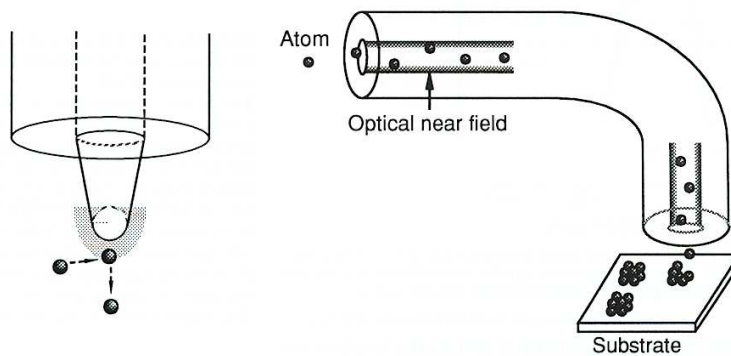
Figure 119: Proposal to trap single atoms in the optical field at the end of a near-field probe (left) or to "nano-deposit" clusters of atoms with hollow-core optical fibers. [from Ohtsu, "Near-field Nano/Atom Optics and Technology"]

145

4.6 SNOM applications

The possible optical resolution far below the optical wavelength, possible down to few nanometers, makes SNOM very attractive for a number of applications. Here, we provide a few examples:

Biology/Chemistry: Ultra-high resolution microscopy and spectroscopy with single molecules, investigation of chemical processes on the nanometer scale, manipulation of single molecules, ...
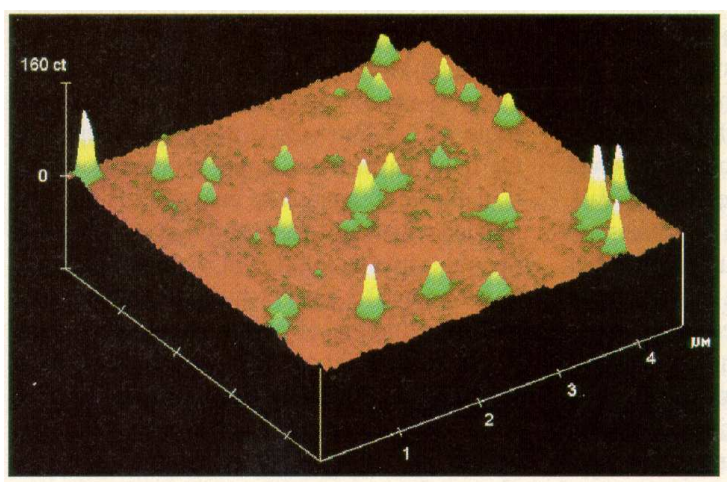
Figure 120: SNOM image of single Oxazin 720 molecules. The optical resolution in this image is approx. 100 nm.
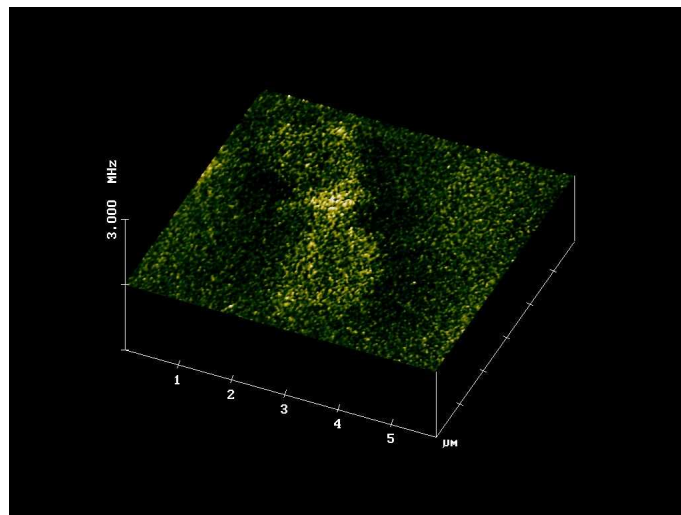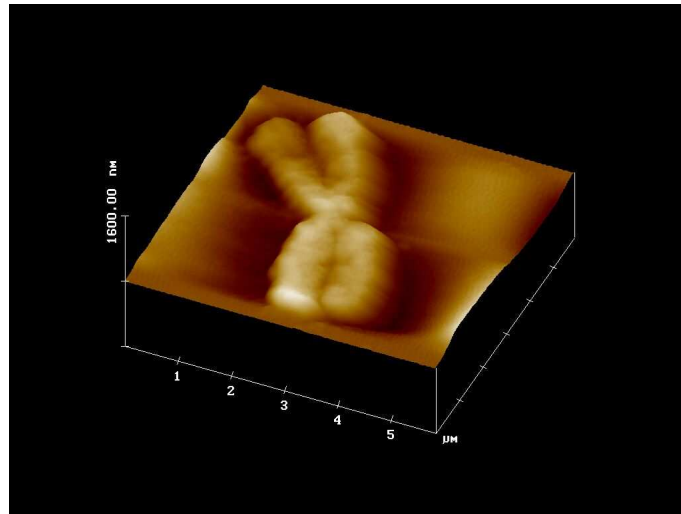
Figure 121: SNOM topography (top) and fluorescence of a single metaphase chromosome. [from http://www.imb-jena.de/ www_kog/index.html]

147

Material science: Spectroscopy of nanostructures, local excitations, transport measurements, time resolved SNOM measurements at room and cryogenic temperatures, ...
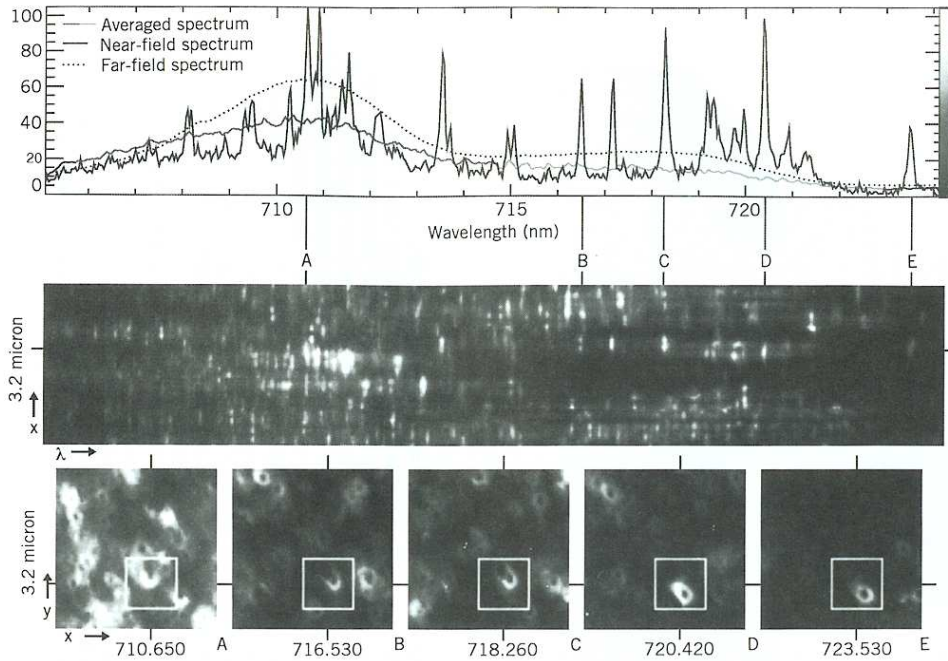
Figure 122: Investigation of localized excitation in a semiconductor quantum film, so-called natural quantum dots with SNOM. a) Near-field spectrum, b) near-field image, c) spectrally filtered near-field [from Hess et al., Science 264, 1740 (1994)]

Optical Data Storage: Storage of information with highest density, development of parallel SNOM applications, ...
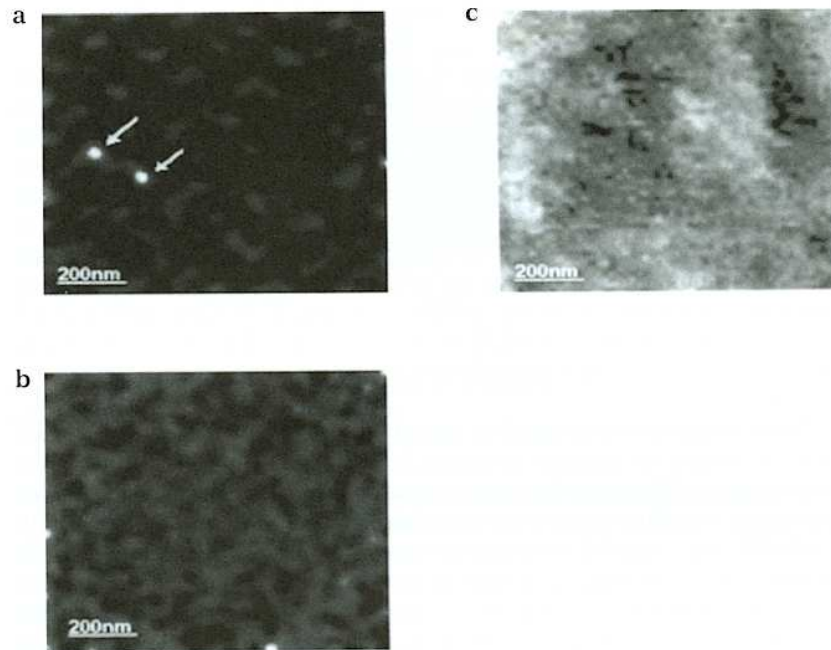
Figure 123: SNOM images a) and b) as well as topography c) of a polystyrene film containing NTI-molecules. Writing of two points using an Ar-ion laser (488 nm) and erasing with a He-Ne laser was demonstrated. [from Kawata, "Nano-Optics"]

Characterization of optical microsystems: Investigation of the optical properties of new micro- and nano-photonic systems and devices, e.g., Photonic Bandgap Structures, PBG (see later chapter).
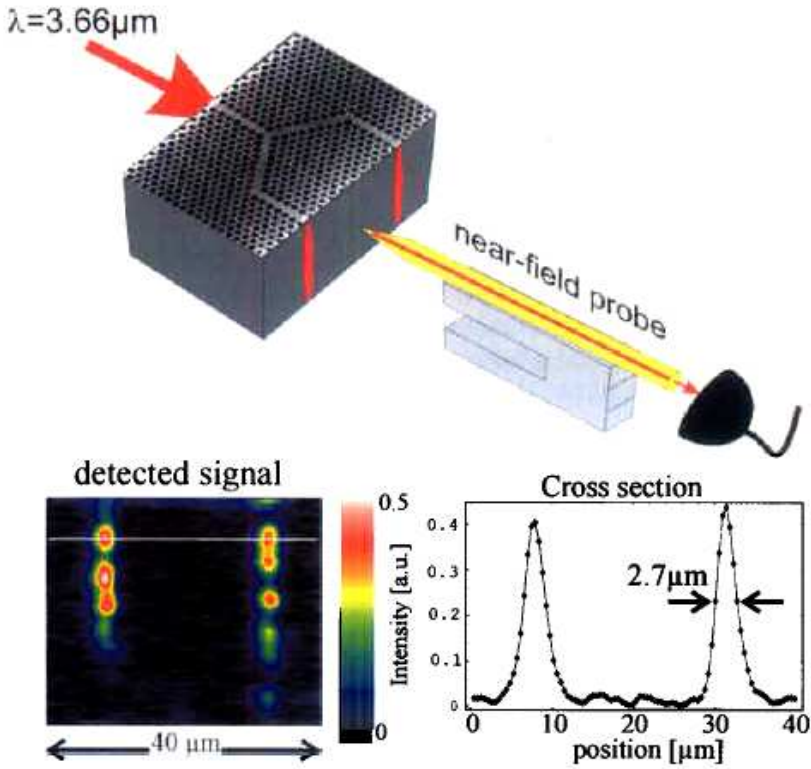
Figure 124: Investigation of the optical performance of a photonic crystal structure with a SNOM probe. [from V. Sandoghdar, "Trends and Developments in Scanning Near-field Microscopy"